



Modeling the atmospheric transport and outflow of polycyclic aromatic hydrocarbons emitted from China

Yanxu Zhang^{a,1}, Huizhong Shen^a, Shu Tao^{a,*}, Jianmin Ma^b

^aLaboratory for Earth Surface Processes, College of Urban and Environmental Sciences, Peking University, Beijing 100871, China

^bAir Quality Research Division, Science and Technology Branch, Environment Canada, 4905 Dufferin Street, Toronto, Ontario M3H 5T4, Canada

ARTICLE INFO

Article history:

Received 2 October 2010

Received in revised form

28 February 2011

Accepted 2 March 2011

Keywords:

PAH

Atmospheric transport model

Outflow flux

CanMETOP

ABSTRACT

An Euler atmospheric transport model CanMETOP (Canadian Model for Environmental Transport of Organochlorine Pesticides) was applied to the atmospheric transport and outflow of polycyclic aromatic hydrocarbons (PAHs) in China in 2003 based on a square kilometer resolution emission inventory. The reaction with OH radical, gas/particle partition by considering the adsorption onto total aerosol surface area, and dynamic soil/ocean–air exchange of PAHs were also considered. The results show that the spatial distribution of PAH concentration levels in the atmosphere is greatly controlled by emission and meteorological conditions. Elevated concentration levels are predicted in Shanxi, Guizhou, North China Plain, Sichuan Basin and Chongqing metropolitan areas due to the high emission densities at those locations. High concentrations are also modeled in environments offshore of China and in the western Pacific Ocean. The model also predicts a slightly decreasing vertical profile in the planetary boundary layer (lower than ~1 km), but concentration decreases ~2 orders of magnitude in the free atmosphere. The Westerlies as well as the East Asian Monsoon and local topographical forcings are identified as key factors influencing the transport pattern of PAHs in China. In 2003, ~3800 tons of the sixteen parent PAHs listed on USEPA priority control list were transported out of China with about 80% transported through the eastern boundary. The outflow concentrates near 30°N, signifying a slight discrepancy from the position of emission density peaks. The center of the outflow plume is located at a height of ~1 km at 120°E, and climbs to 3.5 km and 5 km at 130°E and 140°E, respectively. A seasonal variation of 5–6 fold is also found for the outflow flux with greatly elevated transport flux in spring and winter.

© 2011 Elsevier Ltd. All rights reserved.

1. Introduction

As the world's largest emitter (Zhang and Tao, 2009), China suffers from severe atmospheric PAH pollution. High concentrations of PAHs were extensively detected (Liu et al., 2007), and elevated lung cancer risk is induced among Chinese population due to inhalation exposure of PAHs (Zhang et al., 2009). In addition to domestic risk, as one of the sixteen substances listed in the Convention on Long-range Transboundary Air Pollution Protocol on Persistent Organic Pollutants (United Nations Economic Commission, http://www.unece.org/env/lrtap/pops_h1.htm), the outflow of PAHs from China is also of international concern. Extensive monitoring studies have shown that the PAHs emitted by China can undergo long-range transport and significantly enhance the near

ground concentrations in surrounding countries and continents located downwind of China, including Korea, Japan, and North America under certain meteorological conditions (Lee et al., 2006; Killin et al., 2004; Primbs et al., 2007; Tamamura et al., 2007; Yang et al., 2007; Lang et al., 2008). However, qualitative analysis of the outflow flux of PAHs from China is generally missing in the literature except for a rough estimate by Lang et al. (2008) with a statistical trajectory approach and highly simplified transport and chemistry schemes.

Great diversity exists for PAHs emission density as well as climatological and meteorological conditions in different parts of China (Zhang et al., 2008; Zhang, 1991). Therefore, the transport patterns of PAHs are anticipated to have great variance. For example, Lang et al. (2007) modeled the transport of PAHs emitted from Guangdong, China and found that there is a main transport pathway to the South China Sea and Southeast Asian countries in winter and a main transport pathway to northern mainland China in summer. In another study, Liu et al. (2007) found that eastward and southward transport routes are the main transport pathways for the PAHs emitted from the North China Plain.

* Corresponding author. Tel./fax: +86 10 62751938.

E-mail address: taos@urban.pku.edu.cn (S. Tao).

¹ Department of Atmospheric Sciences, University of Washington, Seattle, WA 98195, United States

Modeling studies for the transport and fate of PAHs were conducted both in regional (Matthias et al., 2009; Prevedouros et al., 2008; Lang et al., 2008; Zhang et al., 2009) and global scale (Sehili and Lammel, 2007; Lammel et al., 2009) with multicompartiment (multimedia) and atmospheric chemistry and transport models. These studies focus on the influence of gas/particle partitioning of PAHs and typically use Benzo[a]pyrene or other selected compounds as the reference chemical. In addition, several studies have addressed the atmospheric transport and outflow of pollutants other than PAHs emitted from East Asia (Liu et al., 2003; Liang et al., 2004; Liang et al., 2005). For instance, Liang et al. (2004) summarized the main outflow mechanisms for CO emitted from East Asia by lifting through convection and the warm conveyor belt followed by a fast transport in the free atmosphere.

In this study, we used a regional scale PAH transport model with a relatively high spatial resolution ($24 \text{ km} \times 24 \text{ km}$) to model the atmospheric transport and fate of PAHs in China. The main objectives are 1) to conduct a comprehensive investigation of the atmospheric transport patterns of PAHs in China, and 2) to quantitatively evaluate the outflow of PAHs from China, with special emphasis on the flux estimate as well as its source location and seasonal variation.

2. Methodology

A modified version of the CanMETOP was used to model the transport and outflow of PAHs (Ma et al., 2003). The details of this model have been presented previously (Ma et al., 2003 and cited references). Briefly, the model has a horizontal spatial resolution of $24 \text{ km} \times 24 \text{ km}$ with 210×270 grids and covers the entirety China and surrounding regions (Fig. 1). The model has 12 vertical layers centered at 1.5, 3.9, 10, 100, 350, 700, 1200, 2000, 3000, 5000 and 7000 m, respectively. Three dimensional atmospheric advection and eddy diffusion are solved numerically by a finite-difference approximation and operator-splitting scheme. An advanced boundary layer parameterization scheme and a non-local turbulence closure are employed to calculate boundary layer height and other related parameters. The dry deposition of particulate matters associated PAHs is assumed to occur at the bottom 4 layers, while the dry deposition velocity is calculated by a series-of-resistances approach. On the contrary, the wet deposition occurs in the whole atmospheric column based on the archived total precipitation data. Due to the short lifetime of PAHs in the atmosphere (Hafner et al., 2005), the contribution of sources from other regions are negligible compared with that from local Chinese sources. Therefore, a zero concentration boundary condition is used in this simulation following Matthias et al. (2009).

The modeled compounds include the sixteen PAHs in the USEPA priority control list, including naphthalene (NAP), acenaphthylene (ACY), acenaphthene (ACE), fluorene (FLO), phenanthrene (PHE), anthracene (ANT), fluoranthene (FLA), pyrene (PYR),

benz(a)anthracene (BaA), chrysene (CHR), benzo(b)fluoranthene (BbF), benzo(k)fluoranthene (BkF), benzo(a)pyrene (BaP), dibenz(a,h)anthracene (DahA), indeno(1,2,3-cd)pyrene (IcdP), and benzo(g,h,i)perylene (BghiP). The total concentration of the 16 PAHs is denoted as PAH16. Among them, BaP was chosen as a representative compound to discuss the general transport and outflow pattern because BaP is the largest contributor to the national total lung cancer risk associated with inhalation exposure of PAHs in China in 2003 (Zhang et al., 2009). BaP's contribution to lung cancer risk was evaluated based on a set of BaP equivalent toxicity factors derived from an animal experiment by Nisbet and Lagoy (1992).

Because the PAH compounds with intermediate molecular weights are semi-volatile and can adsorb onto the surface of aerosols in the atmosphere, the fraction of particulate associated PAHs is calculated according to the temperature and total aerosol surface area concentration (Pankow, 1987). The PAHs in gaseous and particulate phases are combined into a single tracer in the model to save computation time. This setting implies instantaneous partition equilibrium between these two phases and may slightly alter the lifetime of PAHs in each phase; but the influence on the total PAHs should be minimal. The chemical reaction of gas phase PAHs with OH radical is considered and second-order degradation kinetics is assumed for the reaction. The reaction of PAHs with other oxidants, such as NO_3 and O_3 were neglected due to their minor contributions (Prevedouros et al., 2008; Lammel et al., 2009). The degradation of particulate phase PAHs was also neglected because of the lack of experimental data and much smaller reaction coefficient (Estève et al., 2006). The offline monthly mean total aerosol surface area concentration and OH radical number concentrations were collected from the monthly archived data outputted by GEOS-Chem model (http://www-as.harvard.edu/chemistry/trop/geos/geos_hi_res.html). At the bottom level of the atmosphere, the mass transfer flux of gaseous PAHs between air and the underlying soil/water is calculated according to the difference of instantaneous fugacity between air and soil/water. The leaching/sedimentation and degradation of PAHs in soil/water are also modeled dynamically. The modeling details of PAH fate and related parameters are described in the Supporting Information.

A PAH emission inventory with spatial resolution of $1 \text{ km} \times 1 \text{ km}$ was aggregated to $24 \text{ km} \times 24 \text{ km}$ and applied in this study (Zhang et al., 2008). The meteorological and initial concentration data used to drive this model have been described elsewhere (Ma et al., 2003; Zhang et al., 2009). The model was run for the reference year of 2003. In order to evaluate the accuracy of model output for inhalation exposure calculation and lung cancer risk assessment, the annual mean near surface concentrations were carefully compared with observations in our previous study (Zhang et al., 2009). In this study, further comparison with observations from a long time series measurement in Gosan, Korea was conducted and the details are provided in the Supporting Information.

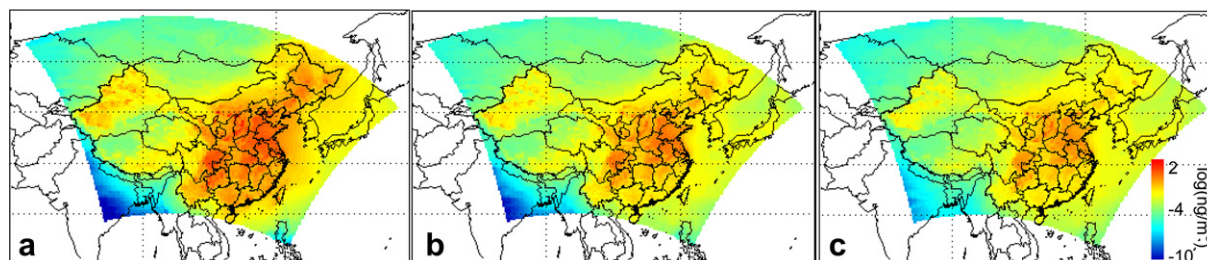


Fig. 1. Near surface atmospheric concentrations of three representative PAHs (from left to right: PHE, CHR and BaP, respectively).

3. Results and discussion

3.1. Surface concentration and vertical profile

Fig. 1 illustrates the annual mean near surface atmospheric concentration of PHE, CHR and BaP, representing volatile, semi-volatile and non-volatile PAHs compounds, respectively. Due to the relatively short lifetime of PAH species, the spatial distribution of PAH concentrations in the atmosphere is dominated largely by local emissions (Hafner et al., 2005). When prevailing westerly winds in the middle and upper troposphere exist over north China, plumes with high levels of PAHs from the Eastern part of China are swept to the East China Sea, the Korean Peninsula, Japan, and further to the western Pacific Ocean. This implies a major eastward transport and outflow pathway. Because of fast degradation, dispersion and deposition, the concentration of PAHs decreases rapidly away from the source regions. For example, BaP concentration is $\sim 1 \text{ ng m}^{-3}$ near the north China seaboard, and subsequently decreases to $\sim 0.1 \text{ ng m}^{-3}$ at $\sim 1000 \text{ km}$ away from the seaboard. Although north winds are dominant near the surface during the wintertime in Eastern China (Zhang, 1991), the meridional wind is much weaker compared to the zonal wind, and no distinct southward plumes can be identified in Fig. 1.

Fig. 2 shows the vertical profiles of PAH concentrations in China. As seen, PAH mixing ratios decrease by a factor of ~ 2 within the planetary boundary level (PBL) compared with mixing ratios near the surface, but sharply decrease in the free troposphere. The vertical profiles of the concentrations of PAHs in both particulate and gaseous phases exhibit a similar pattern, but the former decreases much slower than the latter. This can be attributed to the lower temperatures at higher altitudes, and that PAHs tend to condense into particulate phase and become more persistent to OH radical degradation. An observation conducted in Beijing at a meteorological tower with a height of $\sim 300 \text{ m}$ also shows a similar decreasing trend for both particulate and gaseous PAHs from near the ground (Tao et al., 2007). Up to now, the measurements for the vertical profile of PAH concentrations are rather limited, especially in the free troposphere. So, the model results can supplement the observations with more details about the vertical profile.

3.2. Atmospheric transport of PAHs

The horizontal and vertical transport fluxes were calculated by multiplying concentrations and wind speeds. Fig. 3a shows the annual average horizontal transport fluxes of BaP at the top of the PBL ($\sim 1200 \text{ m}$). With a national mean of $125 \text{ pg m}^{-2} \text{ s}$, the transport

fluxes are much higher near the North China plain, due to the high emission density there (Zhang et al., 2008). Besides, the transport flux is also elevated on the East China Sea and the western Pacific Ocean due to increased winds over the ocean compared to land. On the other hand, due to the much weaker vertical wind speed, the mean vertical transport flux at $\sim 1200 \text{ m}$ was $\sim 0.02 \text{ pg m}^{-2} \text{ s}$ (Fig. 3d, positive/negative means upward/downward transport). Significant upward and downward transports occur on the upwind and downwind sides of Taihang Mountain, respectively (Fig. 3d). A similar pattern can be identified near Wulin Mountain. Due to the relatively smaller spatial scale of these vertical motions, these features were not distinct in the coarse models (Liu et al., 2003). Although the Tibetan Plateau exerts a great influence on the atmospheric general circulation (Zhang, 1991), it is not distinct on Fig. 3d because of the extremely low PAH concentrations surrounding the mountain (Fig. 1).

Significant seasonal variation exists for the atmospheric transport patterns. In summer (June, July and August, Fig. 3b and e), the southerly and southwesterly monsoon flows dominate eastern China equatorward of $\sim 40^\circ \text{N}$. In combination with the Westerlies over northern China, PAHs are transported toward the northeast. Meanwhile, the decreasing trend in altitude from southeast China (Sinomaps, 2005) generates a downward transport in the North China Plain (Fig. 3e). The average horizontal and vertical transport fluxes in summer are about $50 \text{ pg m}^{-2} \text{ s}$ and $-0.1 \text{ pg m}^{-2} \text{ s}$, respectively. In winter (December, January and February, Fig. 3c, f), under the influence of the Siberian High pressure center (Zhang, 1991), the prevailing wind directions in eastern China are northwest ($> 15^\circ \text{N}$) and northeast ($< 15^\circ \text{N}$), respectively. This wind pattern delivers a large portion of PAHs emitted from north China southeastward and southwestward, respectively (Liu et al., 2007). Similarly, the increasing trend in altitude toward Southeast China lifts the north wind and causes strong ascending transport in a large area, including the North China Plain, the southeast seaboard and the offshore environment of China, and even part of the western Pacific Ocean (Fig. 3f). The average horizontal and vertical transport fluxes in winter are about $285 \text{ pg m}^{-2} \text{ s}$ and $0.15 \text{ pg m}^{-2} \text{ s}$, respectively. These fluxes are much higher than those in summer and attributable to much stronger wind speeds and higher anthropogenic PAH emissions in the wintertime (Zhang, 1991; Zhang and Tao, 2008).

The meridional-mean meridional and zonal-mean zonal transport fluxes at different altitudes are presented in Fig. 4. As seen at this figure, the strongest transport flux is near 120°E , 33°N at a height of $\sim 3000 \text{ m}$, where the strong wind speeds compensate decreasing concentrations compared to concentrations near the surface. Overall, south- and eastward transport dominate, which are associated with the East Asian Winter Monsoon and the Westerlies (Zhang, 1991). A much weaker north- and westward transport are modeled in the southeast China ($18\text{--}36^\circ \text{N}$, near 100°E) in the PBL, showing the influence of the summer monsoon in south China (Zhang, 1991).

3.3. Atmospheric outflow of PAHs

3.3.1. Outflow flux estimate

Significant amounts of PAHs are transported out of China, most of which are through the eastern boundary (Lang et al., 2007). Based on the result of this study, there is ~ 3800 tons of PAH16 (accounting for $\sim 3\%$ of the total emission from China) carried out of China through atmospheric transport, and about 80% came through the eastern boundary (an imaginary wall located at 120°E , $18^\circ\text{--}54^\circ \text{N}$, and from the surface to a height at 7000 m).

Fig. 5a presents the comparison of BaP outflow flux across the eastern boundary at different latitudes with BaP emission density.

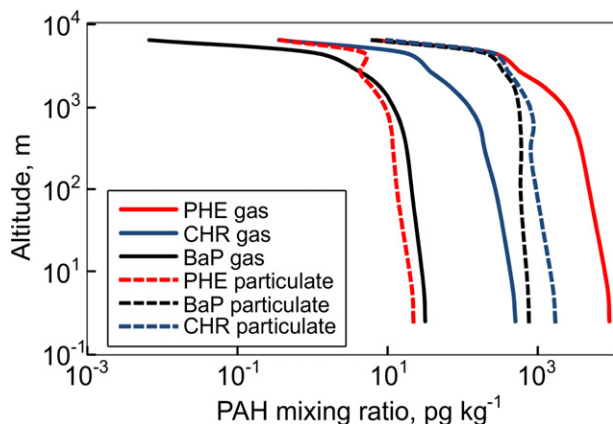


Fig. 2. Vertical profile for the annual mean mixing ratios of three representative PAHs (PHE, CHR and BaP) for both the gaseous and particulate phases.

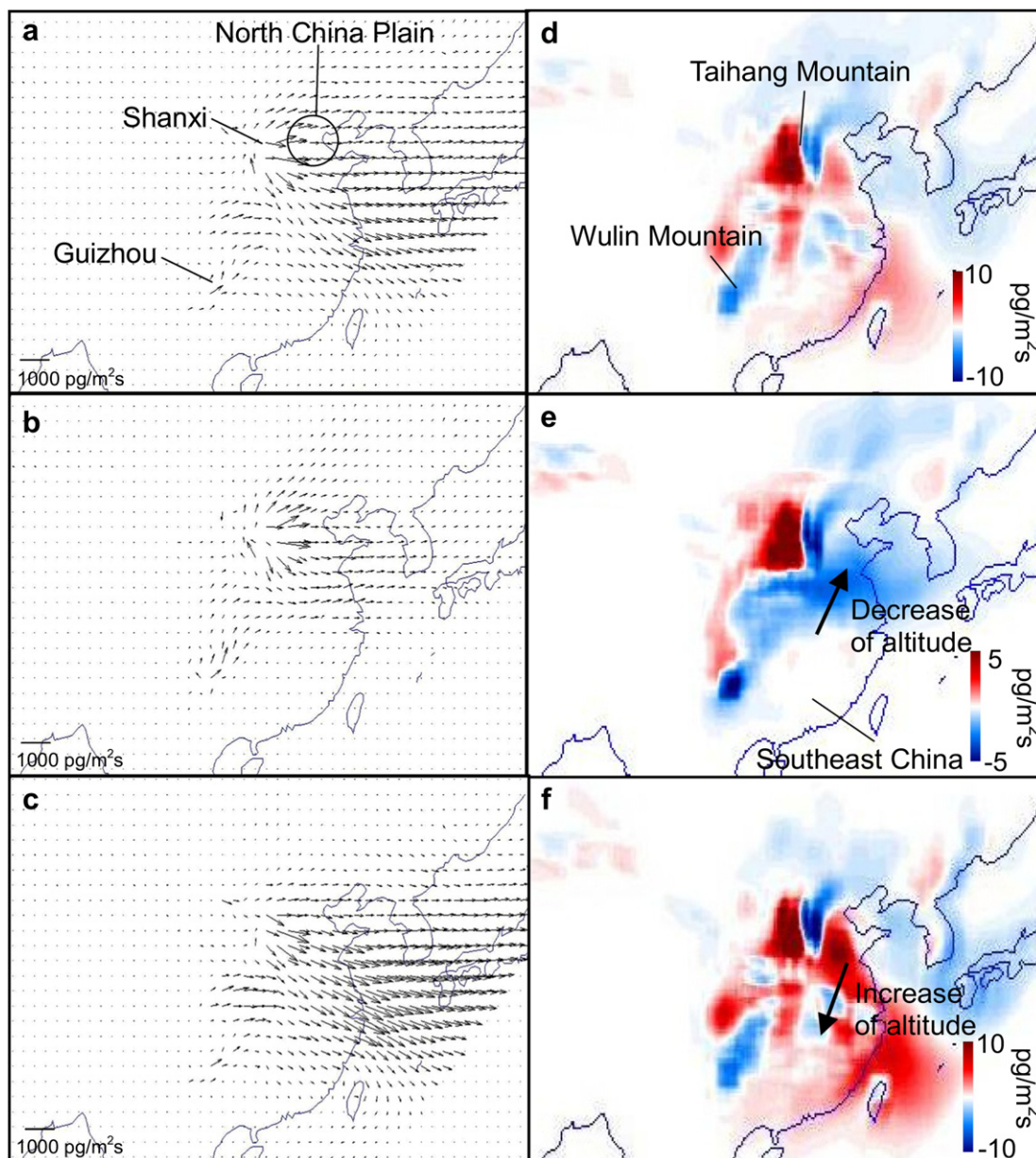


Fig. 3. Average horizontal (a–c) and vertical (d–f) transport fluxes for BaP in summer (June, July and August, b and e) and winter (December, January and February, c and f), and the total year (a, d). For the vertical transport flux, positive (negative) values mean upward (downward) transports.

The peaks of the emission density are located at about 39°N and 26°N, near Shanxi and Guizhou. These provinces have intensive small-scale coke productions. Elevated emission density also exists between 31°N and 40°N, indicating two high emission density regions in the North China Plain as well as the Sichuan Basin and the Chongqing metropolitan area (Zhang et al., 2008). The total BaP outflow flux in this section is $\sim 290 \text{ t yr}^{-1}$ with two peaks near 30°N. The flux decreases toward the north and south borders of China. Generally, the outflow flux greatly concentrates at 27–40°N, and the outflow in this latitudinal band contributes to more than 80% of the total outflow flux in China. This suggests the best sampling locations for capturing the outflow plume of PAHs from China, where intensive measurements, especially aircraft observations in the free atmosphere, are extremely helpful to quantify the outflow flux.

It is necessary to mention that this estimate is based on a single year (2003) study which was subjected to significant interannual

variability. Liu et al. (2003) found that the frequency of cold surges across China associated with the Southern Oscillation Index is the key factor influencing the interannual variability of outflow of CO from East Asia. The outflow was enhanced during La Niña episodes while depressed over El Niño episodes. Liang et al. (2005) proposed that the Asian outflow corresponds to the average sea level pressure over Northeast Asia, which is associated with cyclogenesis in East Asia. Besides, the continuous weakening of the East Asian winter monsoon since the late 1980s also contributes to the interannual variability (Nakamura and Izumi, 2002). However, the basic flow pattern and outflow mechanism stay more or less unchanged.

In a previous study, we have estimated an uncertainty of roughly a factor of 2 for the near surface concentration by considering the uncertainties of emission density, OH radical and aerosol surface area concentration and dry deposition velocity (Zhang et al., 2009). This uncertainty is also applicable to the outflow flux in this study.

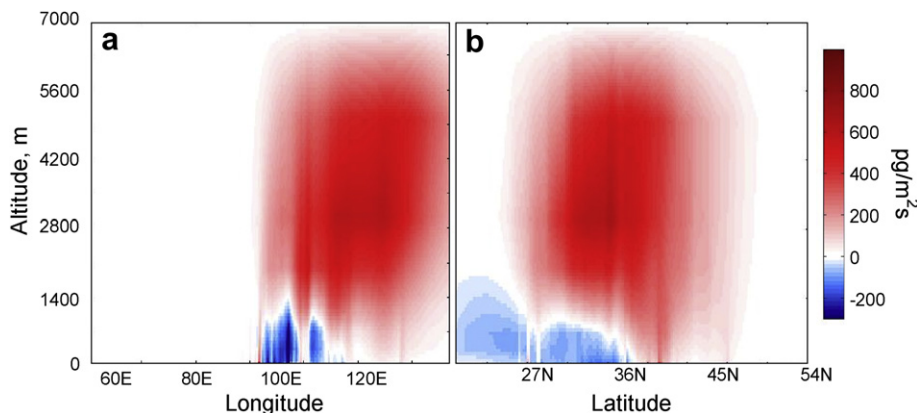


Fig. 4. The annual meridional-mean meridional (a) and zonal-mean zonal (b) transport flux for BaP at different altitudes. Red colors denote east- and southward transport, blue colors denote west- and northward transport, and white color denotes nearly zero transport flux. (For interpretation of the references to colour in this figure legend, the reader is referred to the web version of this article.)

Moreover, the lack of experimental results and the simplification of several key processes for PAH transport and fate also contribute to the overall uncertainty of outflow flux estimate. Based on the parameterization of Lammel et al. (2009), the removal of PAHs by OH radical in daytime contribute about 70%, 20% and 40% for ANT, FLT and BaP, respectively, to the total degradation. The neglecting of NO₃ and O₃ degradation in this study caused an overestimate of the lifetime of PAHs and thus outflow flux, especially during the nighttime. Another important source of uncertainty is the gas/particle partition of PAHs. The model calculated the spatial distribution of seasonal mean particulate phase fraction for three representative PAHs (PHE, CHR and BaP) which are provided in the Supporting Information. In this study, we employed the parameterization by Pankow (1987), which predicts a significantly lower particle-bound fraction of semi-volatile PAHs rather than taking into account both the adsorption onto black carbon (BC) and absorption into organic matters (OM) (Lammel et al., 2009). Although these model settings gave reasonable results overall in comparison with observations (Zhang et al., 2009), the neglecting of high-affinity BC and OM to the gas/particle partition predicts a shorter residence time of PAHs in the atmosphere due to the overestimation of the gaseous fraction exposure to fast chemical degradation (Lammel et al., 2009). This thus indicates an underestimation of the outflow flux of PAHs in this study, and the adsorption onto BC and absorption into OM should be

included in future studies. As the mechanism of gas/particle partitioning of PAHs is still not well understood and open to discussion (Lohmann and Lammel, 2004), more experimental studies and field observations, especially focusing on the association between the partition dynamics and the characteristics of the aerosols, including size, chemistry composition, aging, etc. are required to give more reasonable parameterizations of this process.

3.3.2. Outflow from different regions of China

Due to the great variance of emission density as well as meteorological and climatological conditions, the transport and outflow of PAHs from different regions of China are quite different and were evaluated by a tagged emission approach. The PAH emissions from China were tagged to different tracers based on the geographic location, emission density and topographic conditions (R1–8, shown in Fig. 6a). Fig. 6 also illustrates the transport and outflow patterns of the PAHs emitted by different regions of China. Although the absolute outflow flux has great uncertainty, the transport patterns and the relative contributions from different regions are more accurate.

On an annual basis, R4, R2, R5, R3, R6 and R1 contributed about 33%, 32%, 10%, 6.8%, 5.1% and 4.2% to the total outflow of BaP from China, respectively, while the rest of the source regions only contributed about 7.6% to the total outflow flux. The BaP in R2 (mainly including the North China Plain) is transported eastward

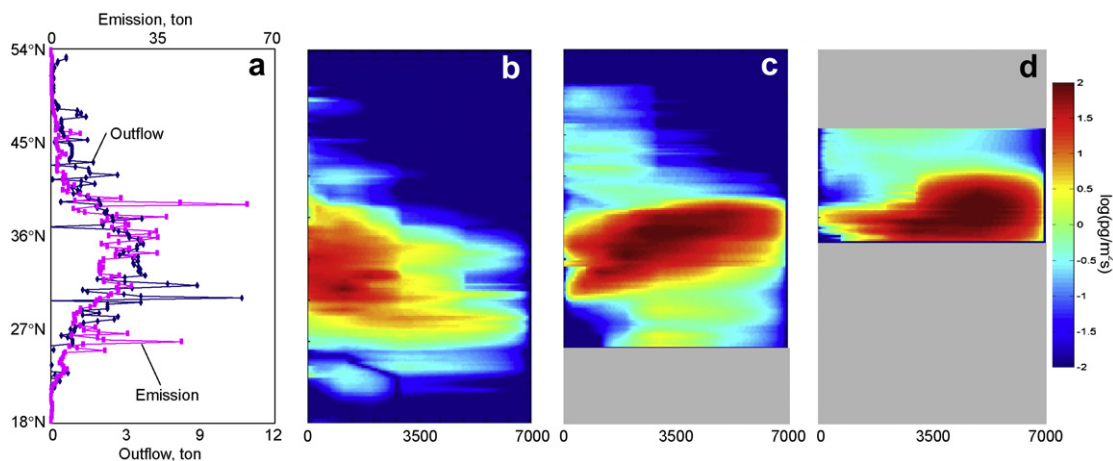


Fig. 5. The variation of outflow flux for BaP: a) the outflow flux at different latitudes compared with that of emission density; b, c, and d) the zonal transport flux cross sections at 120°E, 130°E and 140°E, respectively. The concentration information in the lower portion of c (south of ~25°N) and upper and lower portions (gray shaded area, north of 47°N and south of 35°N, respectively) in d are outside of the model domain, however the center of the outflow plume was captured.

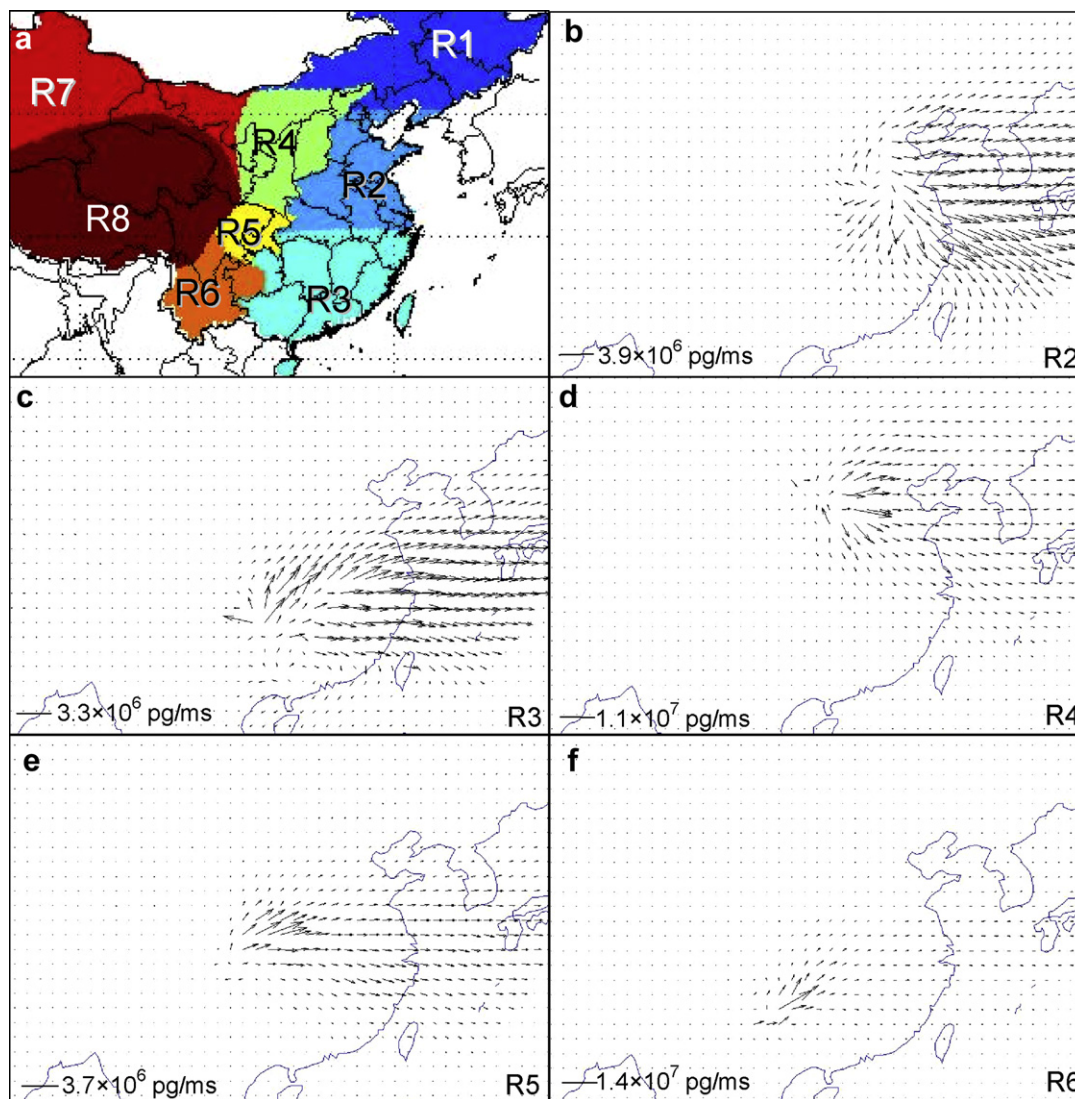


Fig. 6. Transport and outflow pathways of the sum of the gaseous and particulate phase BaP from different regions of China, (a) the tagged emission regions, (b–f) transport pathways of BaP emitted from R2–6, respectively.

directly to the western Pacific. However, frequent occurrences of cold surges from Siberia and Mongolia during the winter season push a large portion of BaP southward up to 30°N and lift the chemicals to a higher atmospheric level where they are subsequently delivered by stronger westerly winds to the west Pacific. Liu et al. (2007) has extensively investigated the transport pathways of PAHs in this region by a forward trajectory clustering approach without considering the removal processes during transport, and divided the trajectories into three groups. The transport occurred mainly in two modes: zonal and meridional, which correspond to the eastward and the southward transport, respectively. Although only qualitative, the analysis by Liu et al. (2007) helps to explain the peak of outflow that appears at about 30°N , where the emission density is not the highest in China. A similar situation takes place in R4 (mainly including the Shanxi province and surrounding areas), although this region is farther from the eastern boundary, strong zonal winds at the lower troposphere associated with southward penetration of the polar front during the wintertime carry a large quantity of PAHs out of China. In this case, the outflow flux was almost evenly distributed between 30° and 40°N . As the PAH emission from Shanxi province is dominated by small-scale coke production (Zhang et al., 2008), the emission control over this industry could not only benefit the local

environment (Zhang et al., 2009), but also mitigate the outflow flux of PAHs from China.

Different from the south- and east-ward transport in northern China, a northward transport occurs in south China on an annual basis (R3, R5 and R6). Although located south of 30°N , the BaP emitted from R3 was transported north of 30°N in the PBL and flowed toward the western Pacific thereafter. Strong transport and outflow fluxes are found north of 30°N . Lang et al. (2007) also found that the PAHs emitted from Guangdong (in R3 in this study) are primarily transported northward in summer and southward in winter. Approximate symmetrical dispersion plumes were found north and south of Guangdong on an annual mean map. For R5 and R6 (including the entire Yunnan province and part of the Sichuan and the Guizhou provinces), although there are large emission densities and strong atmospheric transport near the source region, the outflow flux is generally smaller than R2 and R4 due to the significant distance between R5 and R6 and the boundary of China.

3.3.3. Transport of PAHs in the western Pacific

Fig. 5b–d illustrate the vertical structure of the outflow plume by a series of latitude–altitude cross sections at 120°E , 130°E and 140°E , respectively. As seen in this figure, the outflow is strongest at about

27°–36°N from the surface to ~3500 m at 120°E. The high transport flux near the surface shows that transport in the PBL during the cold season is an important outflow pathway near source regions, especially poleward of 30°N. Moreover, there is also significant outflow in the mid-upper troposphere, and the high outflow flux band can extend to a height of ~7000 m. The largest outflow flux appears at the top of PBL at about 30°N. This implies large-scale ascending motion and convection near the southeast China seaboard in winter as another important transport pathway for the outflow of BaP from China (Fig. 3f). During the journey of the BaP plume induced by China emission to the east, the center of the plume turns northward over the region bounded by 36°N–40°N and 130°E–140°E, respectively (Fig. 5b–d). Meanwhile, the plume climbs to an altitude of ~3500 m and ~5000 m over this region. This is largely because the northward moving warm air climbs over the cold West Siberia air, and it is expected that this forced large-scale ascending motion would lift the chemical to higher altitudes where the jet stream would transport BaP across the Pacific Ocean in a period of several days (Wallace and Hobbs, 2005; Zhang et al., 2010).

3.3.4. Seasonal variation of outflow flux

Fig. 7 presents the seasonal variation of BaP outflow from the major source regions (R2–6) of China. Generally, the outflow fluxes are much larger in winter and spring than in summer and autumn. The magnitude of outflow flux varies 5–6 fold between a peak of 40 t month⁻¹ in December and a minimum of less than 7 t month⁻¹ in June. Given 1–2 fold seasonal variation of the BaP emission flux (Zhang and Tao, 2008), the meteorological conditions are likely to contribute to the remaining 3–4 fold of variation. The episodic outbreak of cold surges in winter and spring that leads to the southward and eastward transport and penetration into the South China Sea is believed to be the controlling factor for the modeled seasonal variability for BaP outflow (Liu et al., 2003). As seen in Fig. 7, this mechanism is of particular importance for the sources located in north China (e.g. R2 and R4), the outflow fluxes peak during November to April, when the outbreak of cold surges is most frequent (Zhang et al., 1997). In addition, small peaks also exist in July for R2, R3 and R6, where the summer monsoon delivers BaP poleward of ~30°N and the PAHs are transported out of the country by the Westerlies.

4. Conclusions

The spatial distributions of PAH concentration levels in atmosphere are greatly controlled by emission and meteorological conditions. Elevated concentration levels are modeled in Shanxi,

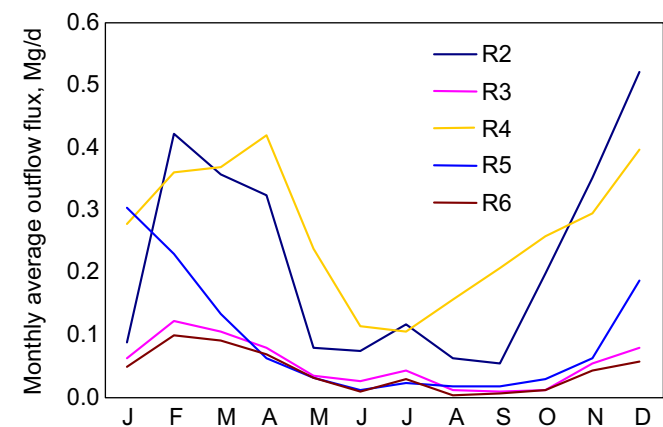


Fig. 7. The seasonal variation of the total BaP outflow from selected source regions in China in 2003.

Guizhou, North China Plain, Sichuan Basin as well as the Chongqing metropolitan area for the high emission density. High concentrations are also modeled at near the China seaboard and the western Pacific Ocean. The model also predicts a slightly decreasing vertical profile in the planetary boundary layer (less than ~1 km), but the concentrations decrease ~2 orders of magnitude in the free atmosphere compared with the level near the surface.

The strongest atmospheric transport of PAHs occurs near the North China Plain and the adjacent areas of the East China Sea and western Pacific Ocean. The Westerlies as well as the East Asian Monsoon and local topographical forcing are also identified as key factors influencing the transport pattern of PAHs in China. Mean meridional and zonal transport flux indicate that the strongest transport occurs at near 120°E, 33°N at a height of about 3000 m. With stronger wind speeds and anthropogenic emissions, the transport flux is largely enhanced in the wintertime.

About 3800 tons of PAH16 were transported out of China in 2003 through atmospheric pathways with about 80% transported through the eastern boundary of China. The outflow concentrates near 30°N, causing a slight discrepancy from the position of emission density peaks. The outflow flux density is highest at a height of ~1 km at 120°E, and keeps climbing to 3.5 km and 5 km at 130°E and 140°E, respectively. A seasonal variation of 5–6 fold is also found for the outflow flux of PAHs in China with greatly elevated transport fluxes in spring and winter.

Acknowledgements

The funding for this study was provided by the National Scientific Foundation of China (40710019001, 40730737), National Basic Research Program (2007CB407303) and the Ministry of Environmental Protection (200809101). The authors gratefully acknowledge Maria Zatzko of the University of Washington for polishing the English of the manuscript.

Appendix. Supplementary material

Supplementary data related to this article can be found online at doi:10.1016/j.atmosenv.2011.03.006.

References

- Estève, W., Budzinski, H., Villenave, E., 2006. Relative rate constants for the heterogeneous reactions of NO₂ and OH radicals with polycyclic aromatic hydrocarbons adsorbed on carbonaceous particles. Part 2: PAHs adsorbed on diesel particulate exhaust SRM 1650a. *Atmospheric Environment* 40, 201–211.
- Hafner, W.D., Carlson, D.L., Hites, R.A., 2005. Influence of local human population on atmospheric polycyclic aromatic hydrocarbon concentrations. *Environmental Science & Technology* 39, 7374–7379.
- Killin, R.K., Simonich, S.L., Jaffe, D.A., DeForest, C.L., Wilson, G.R., 2004. Transpacific and regional atmospheric transport of anthropogenic semivolatile organic compounds to Cheeka Peak Observatory during the spring of 2002. *Journal of Geophysical Research-Atmosphere* 109 (D23). doi:10.1029/2003jd004386.
- Lammel, G., Sehili, A.M., Bond, T.C., Feichter, J., Grassl, H., 2009. Gas/particle partitioning and global distribution of polycyclic aromatic hydrocarbons – a modelling approach. *Chemosphere* 76, 98–106.
- Lang, C., Tao, S., Zhang, G., Fu, J., Simonich, S., 2007. Outflow of polycyclic aromatic hydrocarbons from Guangdong, Southern China. *Environmental Science & Technology* 41, 8370–8375.
- Lang, C., Tao, S., Liu, W., Zhang, Y., Simonich, S., 2008. Atmospheric transport and outflow of polycyclic aromatic hydrocarbons from China. *Environmental Science & Technology* 42, 5196–5201.
- Lee, J.Y., Kim, Y.P., Kang, C.H., Ghim, Y.S., Kaneyasu, N., 2006. Temporal trend and long-range transport of particulate polycyclic aromatic hydrocarbons at Gosan in northeast Asia between 2001 and 2004. *Journal of Geophysical Research-Atmosphere* 111 (D11303). doi:10.1029/2005jd00653711.
- Liang, Q., Jaegle, L., Jaffe, D.A., Weiss-Penzias, P., Heckman, A., Snow, J.A., 2004. Long-range transport of Asian pollution to the northeast Pacific: seasonal variations and transport pathways of carbon monoxide. *Journal of Geophysical Research* 109 (D23S07). doi:10.1029/2003jd004402.

- Liang, Q., Jaegle, L., Wallace, J.M., 2005. Meteorological indices for Asian outflow and transpacific transport on daily to interannual timescales. *Journal of Geophysical Research-Atmosphere* 110 (D18308). doi:10.1029/2005jd005788.
- Liu, H., Jacob, D.J., Bey, I., Yantosca, R.M., Duncan, B.N., Sachse, G.W., 2003. Transport pathways for Asian pollution outflow over the Pacific: interannual and seasonal variations. *Journal of Geophysical Research-Atmosphere* 108 (D20). doi:10.1029/2002JD003102.
- Liu, S., Tao, S., Liu, W., Liu, Y., Dou, H., Zhao, J., Wang, L., Wang, J., Tian, Z., Gao, Y., 2007. Atmospheric polycyclic aromatic hydrocarbons in north China: a winter-time study. *Environmental Science & Technology* 41, 8256–8261.
- Lohmann, R., Lammel, G., 2004. Adsorptive and absorptive contributions to the gas particle partitioning of polycyclic aromatic hydrocarbons: state of knowledge and recommended parameterization for modelling. *Environmental Science & Technology* 38, 3793–3803.
- Ma, J., Daggupaty, S., Harner, T., Li, Y., 2003. Impacts of lindane usage in the Canadian prairies on the Great Lakes ecosystem. 1. Coupled atmospheric transport model and modeled concentrations in air and soil. *Environmental Science & Technology* 37, 3774–3781.
- Matthias, V., Aulinger, A., Quarte, M., 2009. CMAQ simulations of the benzo(a)pyrene distribution over Europe for 2000 and 2001. *Atmospheric Environment* 43, 4078–4086.
- Nakamura, H., Izumi, T., 2002. Interannual and decadal modulations recently observed in the Pacific storm-track activity and East Asian winter monsoon. *Journal of Climate* 15, 1855–1874.
- Nisbet, I.C.T., Lagoy, P.K., 1992. Toxic equivalency factors (TEFs) for polycyclic aromatic-hydrocarbons (PAH). *Regulatory Toxicology and Pharmacology* 16, 290–300.
- Pankow, J.F., 1987. Review and comparative analysis of the theories on partitioning between the gas and aerosol particulate phases in the atmosphere. *Atmospheric Environment* 21, 2275–2283.
- Prevedouros, K., Palm-Cousins, A., Gustafsson, O., Cousins, I.T., 2008. Development of a black carbon-inclusive multi-media model: application for PAHs in Stockholm. *Chemosphere* 70, 607–615.
- Primbs, T., Simonich, S., Schmedding, D., Wilson, G., Jaffe, D., Takami, A., Kato, S., Hatakeyama, S., Kajii, Y., 2007. Atmospheric outflow of anthropogenic semivolatile organic compounds from East Asia in spring 2004. *Environmental Science & Technology* 41, 3551–3558.
- Sehili, A.M., Lammel, G., 2007. Global fate and distribution of polycyclic aromatic hydrocarbons emitted from Europe and Russia. *Atmospheric Environment* 41, 8301–8315.
- Sinomaps, 2005. Atlas of Physical Geography of China. Sinomaps Press, Beijing.
- Tamamura, S., Sato, T., Ota, Y., Wang, X., Tang, N., Hayakawa, K., 2007. Long-range transport of polycyclic aromatic hydrocarbons (PAHs) from the eastern Asian continent to Kanazawa, Japan with Asian dust. *Atmospheric Environment* 41, 2580–2593.
- Tao, S., Wang, Y., Wu, S., Liu, S., Dou, H., Liu, Y., Lang, C., Hu, F., Xing, B., 2007. Vertical distribution of polycyclic aromatic hydrocarbons in atmospheric boundary layer of Beijing in winter. *Atmospheric Environment* 41, 9594–9602.
- Wallace, M.J., Hobbs, P.V., 2005. *Atmospheric Science: an Introductory Survey*, second ed. Elsevier, Burlington.
- Yang, X., Okada, Y., Tang, N., Matsunaga, S., Tamura, K., Lin, J., Kameda, T., Toriba, A., Hayakawa, K., 2007. Long-range transport of polycyclic aromatic hydrocarbons from China to Japan. *Atmospheric Environment* 41, 2710–2718.
- Zhang, J., 1991. *China Climate*. China Meteorological Press, Beijing.
- Zhang, Y., Sperber, K.R., Boyle, J.S., 1997. Climatology and interannual variation of the East Asian winter monsoon: results from the 1979–95 NCEP/NCAR reanalysis. *Monthly Weather Review* 125, 2605–2619.
- Zhang, Y., Tao, S., 2008. Seasonal variation of polycyclic aromatic hydrocarbons (PAH) emissions in China. *Environmental Pollution* 156, 657–663.
- Zhang, Y., Tao, S., 2009. Global atmospheric emission inventory of polycyclic aromatic hydrocarbons (PAHs) for 2004. *Atmospheric Environment* 43, 812–819.
- Zhang, Y., Dou, H., Chang, B., Wei, Z., Qiu, W., Liu, S., Liu, W., Tao, S., 2008. Emission of polycyclic aromatic hydrocarbons from indoor straw burning and emission inventory updating in China. *Annals of the New York Academy of Sciences* 1140, 218–227.
- Zhang, Y., Tao, S., Shen, H., Ma, J., 2009. Inhalation exposure to ambient polycyclic aromatic hydrocarbons and lung cancer risk of Chinese population. *Proceedings of National Academy of Sciences of the United States of America* 106, 21063–21067.
- Zhang, L., Ma, J., Tian, C., Li, Y., 2010. Atmospheric transport of persistent semi-volatile organic chemicals to the Arctic and cold condensation at the mid-troposphere – part 2: 3-D modeling of episodic atmospheric transport. *Atmospheric Chemistry and Physics* 10, 7315–7324.